

Neutrino mass measurement background  
suppression using a predominantly electric E@m  
storage ring

Richard Talman

Laboratory for Elementary-Particle Physics  
Cornell University, Ithaca, NY, USA

BB24, Beam-Beam Effects in Circular Colliders  
EPFL, Zurich, Switzerland, Sep 2-5, 2024

Ref: arXiv:2402.04109v1 [physics.acc-ph]  
JINST\_006P\_0224, Accepted: 27 Aug 2024

## 2 Example of neutrino mass determinations using terrestrial tritium beta-decay.

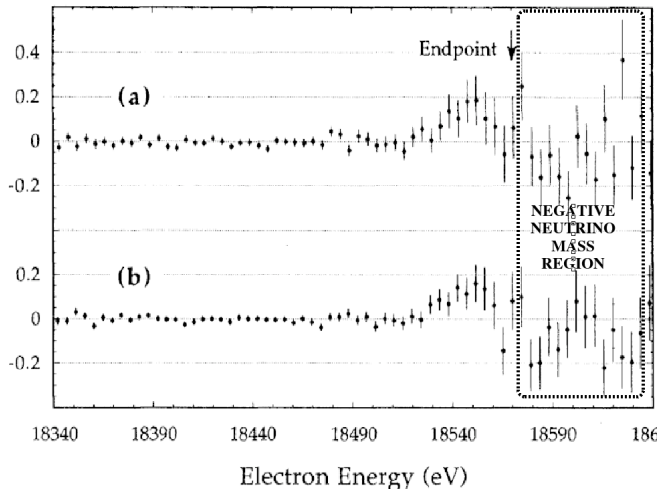


**Figure 1:** Livermore lab Kurie plot for the tritium  $\beta$  decay process,  $t \rightarrow h + e^- + \nu$ . Note the energy-violating  $\beta$ -decay “background” above the electron energy endpoint. [For “MASS” read MASS<sup>2</sup>].

### 3 Chronology of neutrino mass measurement using tritium beta decay

Rep. Prog. Phys. **71** (2008) 086201

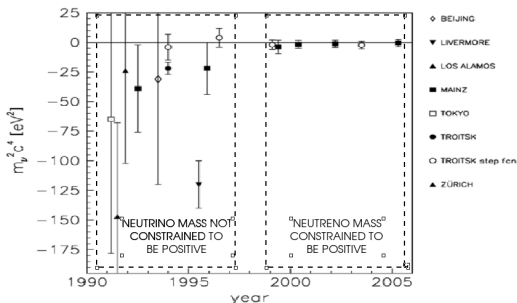


**Figure 1.** Squared neutrino mass values obtained from tritium  $\beta$  decay in the decisive period 1990–2005 plotted against the year of publication (see text for the references). The results from the more recent experiments in Mainz and Troitsk, presented in section 4, are already included.

**Figure 2:** Notice, in particular, the 1996 determination, to  $\pm 6\sigma$  accuracy that the neutrino mass-squared is  $-120 \text{ eV}^2$ ; meaning the mass itself is complex  $\approx \pm 11 i \text{ eV}$ . **Subsequent determinations have “suppressed” the energy-violating counts as “unphysical”.** This strains credulaty, since the energy-violating events seem to mirror the excess energy preserving events

#### 4 PTR superimposed electric + magnetic storage ring bend sector

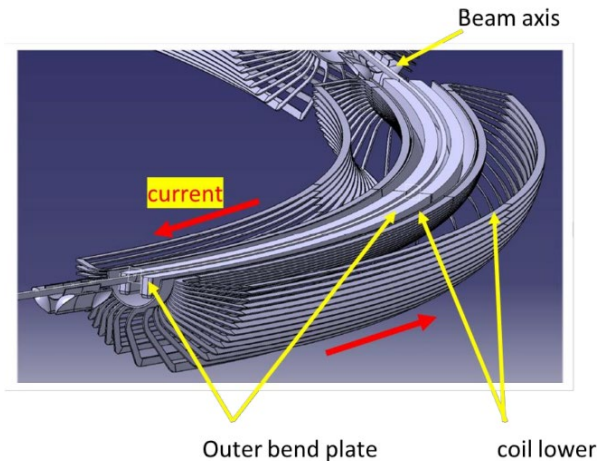


**Figure 3:** Perspective sector mock-up of PTR, a superimposed E&m prototype ring.  $\cos \theta$ -dipoles surround the beam tube, within which are the capacitor plate electrodes. The superimposed coil design is due to Helmut Söltner.

## 5 Description of superimposed electric/magnetic bending

- ▶ To represent a small part of the required bending force at radius  $r_0$  being provided by magnetic bending while preserving the orbit curvature we define “electrical and magnetic bending fractions”  $\eta_E$  and  $\eta_M$  satisfying

$$\eta_E + \eta_M = 1, \text{ where, say, } |\eta_M/\eta_E| < 1/3$$

- ▶ This perturbation “splits” a unique velocity solution into two separate velocity solutions; this enables two different particle types to co-circulate at the same time.
- ▶ As a result there are periodic “rear-end” collisions between two particles co-moving with different velocities in the laboratory, such that their CM KEs are in the several 100 KeV range; i.e. comparable with the Coulomb barrier height.
- ▶ All incident and scattered particles can then have convenient laboratory KEs, two orders of magnitude higher, in the tens or hundreds of MeV range.

## 6 Beam bunching of different velocity beams by a single cavity

BUNCHING of 2 BEAMS of DIFFERENT VELOCITY in SINGLE RF CAVITY

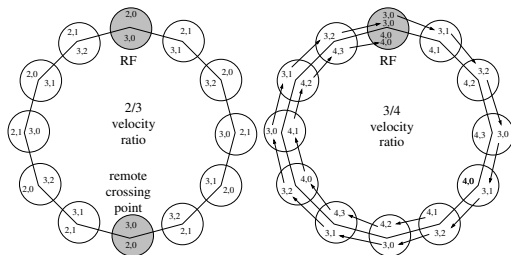
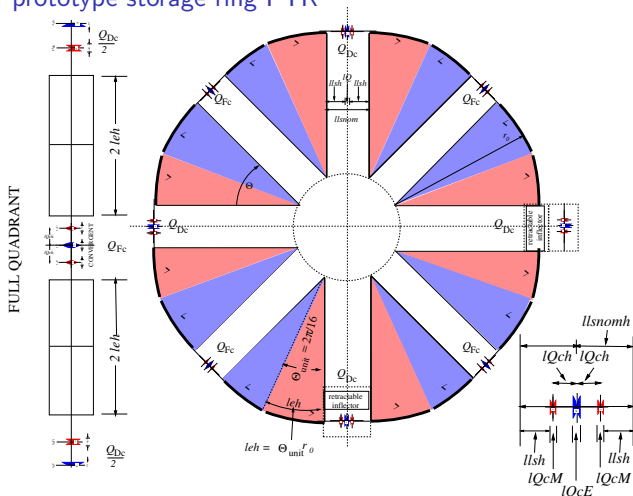


Figure 4: Stable RF buckets for different velocity ratio beams.

- ▶ With 3/4 velocity ratio and  $3 \times 4 = 12$ , the RF frequency can be the 12'th harmonic of a standard base frequency,  $f_{\text{base}}$ , itself a harmonic number  $h_n$  multiple  $f_{\text{base}} = h_n f_{\text{rev}}$ . of the revolution frequency; both circulating beams can be bunched by a single RF cavity (or a pair, centered on the RF) in spite of their different velocities.

## 7 Design of prototype storage ring PTR



**Figure 5:** Lattice layouts for PTR, the proposed prototype nuclear transmutation storage ring prototype; “compromise” quadrupole lower right. The circumference has been taken to be 102 m, but the entire lattice can be scaled, e.g. to reduce peak field requirements.

## 8 PTR optics, super-periodicity=8, Maple:BSM program

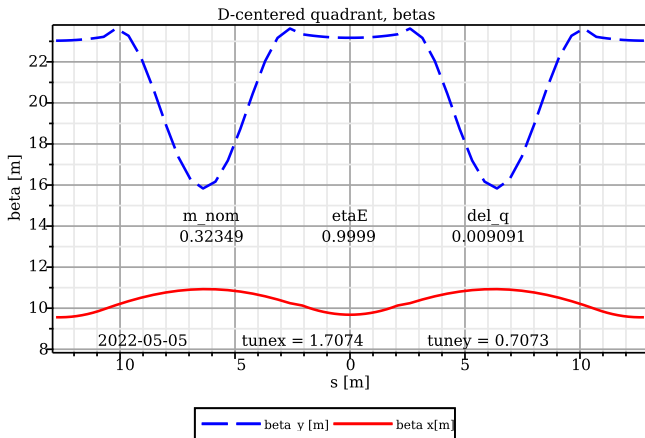


**Figure 6:** Refined PTR tuning, with quad strengths and  $m_{nom.}$  (adjusted to 0.32349) for (distortion-free) equal-fractional-tune,  $Q_x = Q_y + 1$ , operation on the difference resonance. Not counting geometric horizontal focusing, thick lens pole shape horizontal and vertical focusing strengths are then identical. Mnemonic:  $m_{nom.} = 1/3$ .



## 9 “Compromise” work-around for disallowed E&M quadrupole superposition

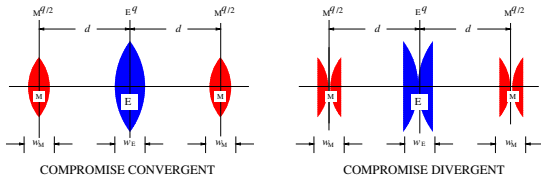


**Figure 7:** “Compromise quadrupole” representation of an electric quadrupole with (weak) magnetic quadrupole superimposed. Blue quads are electric, red magnetic.

- ▶ With magnetic yokes serving also as electrodes, electric and magnetic quads would be relatively skew, **which is unacceptable..**
- ▶ A pair of thin weak magnetic quads can be centered on a stronger electric quad to produce a “compromise” superposition of erect quadrupoles.
- ▶ For beams traveling in the same direction, with the same fractional quad strengths as for the bending, the superimposed E&m quadrupole focal lengths will be nearly the same for both beams.
- ▶ The (horizontal) geometric focusing will also be the same.

# 10 “Compromise” triplets

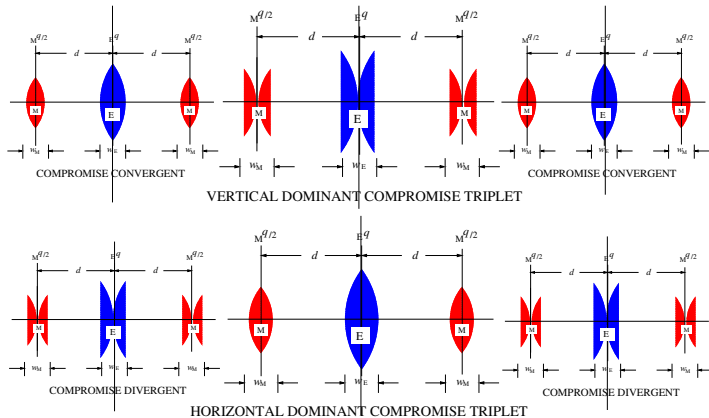


Figure 8: Compromise triplets.

## 11 PTR Rear-End Collider, round beam, low beta (IR) optics

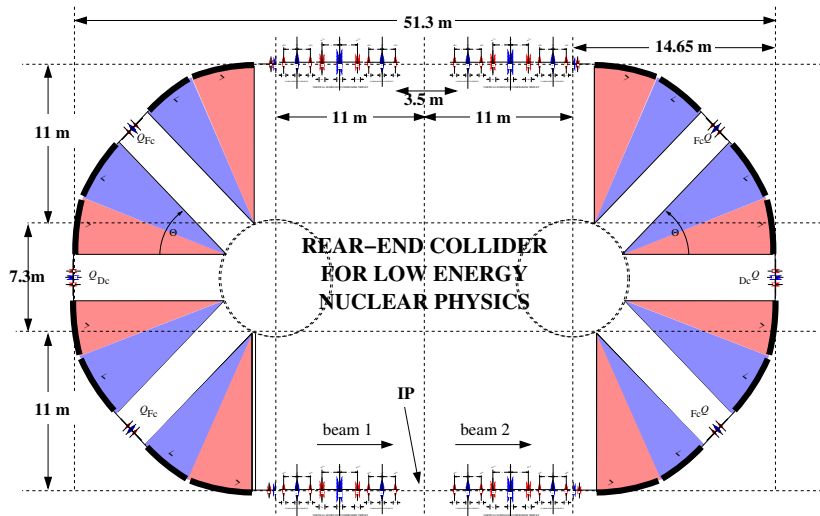
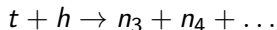


Figure 9: Schematic round beam, low beta optics

## 12 Two body nuclear elastic and “pseudo-elastic” collisions

- ▶ Consider two body elastic and inelastic collisions



- ▶ where, for simplicity, the incident nuclei have been taken to be  
 $n_1 = t(\text{triton}) \equiv {}^3\text{H}_1^+ \equiv 3\text{H}$  and  
 $n_2 = h(\text{helion}) \equiv {}^3\text{He}_2^{++} \equiv 3\text{He}$ .
- ▶ and  $n_3$  and  $n_4$  are the same, or other long-lived isotope nuclei, such as  $p = {}^1\text{H}_1^+$ ,  $d = {}^2\text{H}_1^+$ , or  $\alpha = {}^4\text{He}_2^{++} \equiv 4\text{He}$ , etc.

### 13 Two body collisions (continued)

- ▶ Specializing further, consider elastic two body strong nuclear interaction processes,

$$t + h \rightarrow t + h \quad (1)$$

$$t + h \rightarrow d + \alpha \quad (2)$$

- ▶ or inelastic, weak nuclear reactions (i.e.  $\beta$ -decay processes),

$$t + h \rightarrow t + (t + e^+ + \nu) \quad (3)$$

$$t + h \rightarrow (h + e^- + \nu) + h \quad (4)$$

formally treated as two-body processes,

- ▶ The output state can be treated as two-body, with the parenthesized combination being the second body.
- ▶ For now consider neutrino mass determination in process (3).

## 14 Two body collisions (continued)

- ▶ All such nuclear scattering events can be studied in the PTR ring, with  $t$  and  $h$  beams of different velocity, co-circulating in the same direction, at the same time.
- ▶ Faster beam bunches (say helions) will “lap” the slower triton bunches regularly.
- ▶ Conditions can be controlled such that the resulting rear-end collisions all occur within detection apparatus recording scattering events (1) through (4) at an intersection point (IP).
- ▶ Uniquely special and important about these events is that they occur in a reference frame that is moving with semi-relativistic velocity in the laboratory.

## 15 Typical beam parameters and rear end collision point centering

**Table 1:** Fine-grain scan to center the collision point for co-traveling KE1=31.7 MeV helion kinetic energy and 17.702 MeV triton KE. The bend radius is  $r_0 = 11$  m. CM quantities are indicated by asterisks (\*). Q12 is the sum of CM kinetic energy values which is comparable with the Coulomb barrier potential

bm 1	beta1	KE1 MeV	E0 MV/m	etaM1	beta2	KE2 MeV	beta*	gamma*	M* GeV	Q12 KeV	t,t*bratio 3	bm 2
h	0.1443	29.700	3.96487	-0.47620	0.1082	16.582	0.12628	1.00807	5.61826	945.8	4.00148	t
h	0.1467	30.700	4.10054	-0.47724	0.1100	17.142	0.12836	1.00834	5.61829	977.2	4.00081	t
h	0.1490	31.700	4.23635	-0.47828	0.1117	17.702	0.13041	1.00861	5.61832	1008.6	4.00015	t
h	0.1513	32.700	4.37230	-0.47932	0.1135	18.262	0.13243	1.00889	5.61835	1040.0	3.99948	t
h	0.1535	33.700	4.50839	-0.48036	0.1152	18.822	0.13441	1.00916	5.61838	1071.3	3.99882	t

- ▶ With velocity ratio 4/3, multiplying by t=3 produces the central entry in the second last column, which is close enough to 4 for exact phase locking.
- ▶ While the triton bunch makes three complete revolutions the helion bunch makes four.
- ▶ The electric field value is 4.23635 MV/m (common, obviously, to both beams)
- ▶ The fractional bending factor of the helion beam is  $\eta_{M1} = -0.4782$ . Being negative, the helion bending superposition is “destructive”, with  $\eta_E = 1.4782$ .

## 16 Beam condition reproducibility

- ▶ Incident  $t$  and  $h$  beams can both be nearly 100% polarized
- ▶ Since both magnetic dipole moments (MDM) are known to 9 decimal points, and their Larmor precessions can be stabilized to the same accuracy, the initial state 4-momenta will be known and reproducible to the same accuracy.
- ▶ In the overall CM, the hadron-jet and lepton-jet 3-momenta are equal (but opposite). “Jet” terminology is explained shortly.



## 17 Beam condition reproducibility (cont.)

- ▶ For elastic scattering processes (1) and (2) the kinematics is highly over-determined! And, in any case, the output angles can also be measured quite accurately.
- ▶ For  $\beta$ -decay processes, for example to determine the neutrino mass, it is useful to interpret processes (3) and (4) using perfectly collimated incident state hadron jet, (quite tightly collimated) final state hadron jet, and **almost isotropic** final state lepton jet.
- ▶ The precision with which the neutrino mass can be measured depends on the accuracy with which these constraints can be exploited.

## 18 Storage ring advantages and sensitivity to the neutrino mass

- ▶ Experimentally, since the unscattered triton, call it  $t_1$ , and the scattered triton  $t_2$  are nearly parallel, with accurately known momenta, the 4-momentum of the final state hadron jet will be known to high precision.
- ▶ Our measured  $e^+$  energy and direction provide sufficient further information to establish the entire kinematics with good precision.
- ▶ The event characterization, including neutrino 4-momentum, is too detailed for any “background” to exist.
- ▶ The weak interaction cross section (which is proportional to the neutrino energy), can be much greater than for terrestrial beta decay.

## 19 “Two-body” jet kinematics ( $t + h \rightarrow (t_1 + t_2) + (e^+ + \nu)$ )

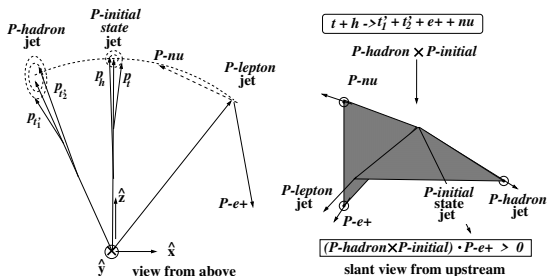


Figure 10: . Jet representation of the nuclear transmutation process.

- ▶ At the low energies of nuclear physics, a convenient rule of thumb for two body kinematics is that, while the center of mass momentum is dominated by the hadrons, (in this case incident state ( $t + h$ ) and final state ( $t_1 + t_2$ )), the kinetic energy is carried primarily by the light particles (in this case ( $e + \nu$ )).
- ▶ The 3-momenta of all three of the jets lie in the same plane.
- ▶ The incident jet is truly “jet-like”—the 3-momenta are exactly parallel.
- ▶ The final state hadron jet is nearly as tightly collimated—laboratory separation angle several degrees.
- ▶ But the lepton jet could scarcely be less “jet-like”—in their own CM the electron and neutrino momenta are isotropic and back-to-back. In the laboratory frame the same is only more or less true.

## 20 Conclusion and extra slides

- ▶ Instead of the single electron signature of terrestrial tritium beta decay, the proposed process produces a clean, background-free detection of both final state electron and hadron, with fully-determined kinematics.
- ▶ Just one of many low energy nuclear measurement goals has been mentioned. Another might be the detection of elastic scattering in which one spin flips while the other does not, would be a violation of time reversal invariance.
- ▶ Thanks for your attention

## 21 Electron-induced, inverse beta decay triton detection apparatus

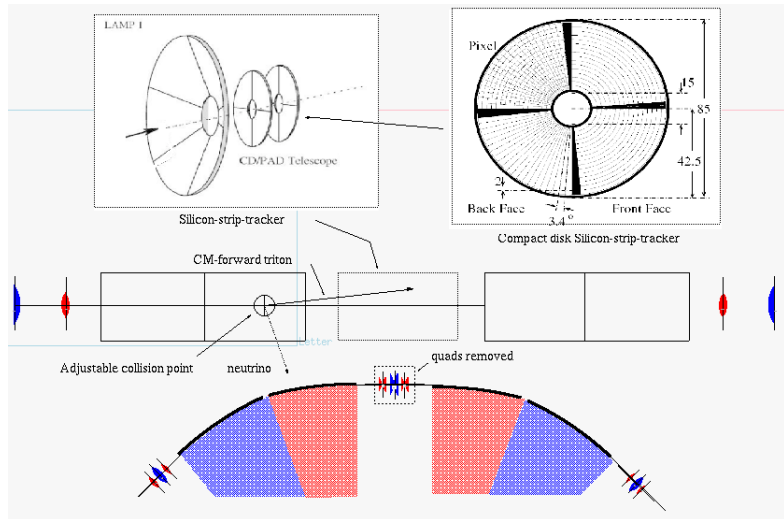


Figure 11: A scattered triton detection, with the triton stopping in a tracking chamber with micron-scale pixel size..

## 22 Rate of electron-induced free-EC tritium beta “reincarnations”

Neglecting low beta intersection region amplification, beam shape variation, injection, maintenance down-time, as well as other inconvenient details, a stripped down rate estimate with optimistic parameters follows; with  $A=3$ , nucleon mass  $M=1$  GeV, electron energy  $\mathcal{E}_e = 0.1$  GeV, ring circumference 100 m; radius of curvature  $r_0=11$  m.

$$\text{storage ring revolution frequency: } f_{\text{sr}} = 3 \times 10^6 \text{ Hz,}$$

$$\text{Fermi constant: } G_F = 1.166 \times 10^{-5} \text{ GeV}^{-2},$$

$$\text{Mandelstam CM-energy-squared. } 2\mathcal{E}_e A M: s = 0.6 \text{ GeV}^2,$$

$$\text{total e,h Fermi cross section, } G_F^2 s / \pi : \sigma_{\text{eh}} = 2.60 \times 10^{-11} \text{ GeV}^{-2},$$

$$\begin{aligned} \text{total e,h Fermi cross section: } \sigma_{\text{eh}} &= G_F^2 s / \pi \\ &= 2.60 \times 10^{-11} \text{ GeV}^{-4}, \end{aligned}$$

$$\text{area unit conversion factor: } 1 \text{ GeV}^{-2} = 0.329 \text{ mb,}$$

$$\text{total e,h Fermi cross section in barn units: } \sigma_{\text{ht}} = 2.81 \times 10^{-12} \text{ mb}$$

$$\text{stored particles in each beam: } N_b = 10^{12},$$

$$\text{beam area: } A_b = 10^{-3} \text{ cm}^2,$$

$$\text{target opacity } N_b \sigma_{\text{eh}} / A_b : O_T = 0.281 \times 10^{-21}$$

$$\text{full ring electron scattering rate } f_{\text{sr}} N_b O_T: \text{rate}_s = 0.84 \times 10^{-4} / \text{second}$$





$$\text{tritium reincarnations per year } \text{rate}[s] \times 3 \times 10^7: \text{rate}[y] = 2530 / \text{year}$$

(1)






## 23 Low mass, charged, free electron (or positron) capture candidates








A	Z	N	S	P	A	Z	N	S	P	A	Z	N	S	P	A	Z	N	S	P		
p	1	H	1	0	1/2+																
d	2	H	1	1	1+																
t	3	H	1	2	1/2+	h	3	He	2	1	1/2+										
	4	H	1	3	2-	$\alpha$	4	He	2	2	0+	4	Li	3	1	2-					
	5	H	1	4	1/2+	5	He	2	3	3/2-	5	Li	3	2	3/2-						
					6	He	2	4	0+	6	Li	3	3	1+	6	Be	4	2	0+		
										7	Li	3	4	3/2-	7	Be	4	3	3/2-		
															8	Be	4	4	0+		
A	Z	N	S	P	A	Z	N	S	P	A	Z	N	S	P	A	Z	N	S	P		





**Figure 12:** Table showing (side-by-side) low mass ( $0 < Z < 5$ ,  $A < 9$ ) candidates for free electron or positron capture  $\beta$ -decay" transmutations. Every entry has at least a multi-year lifetime and can be linac-accelerated to 60 MeV/nucleon energy to produce mA-level average current beams with 1/2 percent energy spread. [Cite Deepak Raparia]

-  I. A. Koop, *Asymmetric energy colliding ion beams in the EDM storage ring*, TUPWO040, Proceedings of IPAC2013, Shanghai, China
-  R. Talman and J. Talman, *Electric dipole moment planning with a resurrected BNL Alternating Gradient Synchrotron electron analog ring*, PRST-AB, 18, 074004, 2015
-  R. Talman, *Superimposed Electric/Magnetic Dipole Moment Comparator Lattice Design*, ICFA Beam Dynamics Newsletter #82, Yunhai Cai, editor, Journal of Instrumentation, JINST\_118P\_0721, 2021
-  R. Talman, *Difference of measured proton and He3 EDMs: a reduced systematics test of T-reversal invariance*, Journal of Instrumentation, JINST\_060P\_0522, 2022
-  R. Talman, *Proposed experimental study of wave-particle duality in  $p,p$  scattering*, <https://arxiv.org/abs/2302.03557>, and Journal of Instrumentation, <https://pos.sissa.it/433/039/pdf>, 2023



-  R. Talman, *Difference of measured proton and He3 EDMs: reduced systematics test of T-reversal Invariance*, Snowmass-Seattle Meeting, <https://indico.fnal.gov/event/22303/contributions/247083>, 2022
-  CPEDM Group, *Storage ring to search for electric dipole moments of charged particles Feasibility study*, CERN Yellow Reports: Monographs, CERN-2021-003, 2021
-  *Proposed experimental study of wave-particle duality in p,p scattering*, Journal of Instrumentation, <https://pos.sissa.it/433/039/pdf>, Chapter 5, “Lattice Design and Performance”.
-  V. B. Reva, *COSY experience of electron cooling*, 12th Workshop on Beam Cooling and Related Topics, COOL2019, Novosibirsk, Russia, JACoW Publishing, doi:10.18429/JACoW-COOL2019-MOX01, 2019
-  E. Fermi, *High Energy Nuclear Events*, Progr. Theor. Physics 5, 570, 1950

-  R. Hagedorn, *Relativistic Kinematics*, W. A. Benjamin, Inc., 1960
-  H. J. Stein et al., *Present performance of electron cooling at COSY*, <https://arxiv.org/pdf/1101.5963>, 2002
-  C. Wilkin, *The legacy of the experimental hadron physics program at COSY*, Eur. Phys. J. A 53 (2017) 114, 2017
-  D. Eversmann et al., *New method for a continuous determination of the spin tune in storage rings and implications for precision experiments*, Phys. Rev. Lett. **115** 094801, 2015
-  N. Hempelmann et al., *Phase-locking the spin precession in a storage ring*, P.R.L. 119, 119401, 2017
-  F. Rathmann, N. Nikoliev, and J. Slim, *Spin dynamics investigations for the electric dipole moment experiment*, Phys. Rev. Accel. Beams 23, 024601, 2020
-  J. Slim et al., *First detection of collective oscillations of a stored deuteron beam with an amplitude close to the quantum limit*, Phys. Rev. Accel. Beams, 24, 124601, 2021

-  F. Rathmann, *First direct hadron EDM measurement with deuterons using COSY*, Willy Haerberli Memorial Symposium, <https://www.physics.wisc.edu/haeberli-symposium>, 2022
-  R. Talman, *Improving the hadron EDM upper limit using doubly-magic proton and helion beams*, arXiv:2205.10526v1 [physics.acc-ph] 21 May, 2022
-  R. Talman and N. N. Nikolaev, *Colliding beam elastic  $p, p$  and  $p, d$  scattering to test  $T$ - and  $P$ -violation*, Snowmass 2021, Community Town Hall/86, 5 October, 2020
-  P. Lenisa et al., *Low-energy spin-physics experiments with polarized beams and targets at the COSY storage ring*, EPJ Techniques and Instrumentation, <https://doi.org/10.1140/epjti/s40485-019-0051-y>, 2019